Characterisation of a room temperature quantum efficient detector for application as a primary standard for radiometry

Katharina Salffner, Philipp Schneider and Saulius Nevas
PTB, Bundesallee 100, 38116 Braunschweig, Germany

1 Introduction

As far back as 1979, Geist et al. proposed that, through advanced knowledge of the physics inside Si photodiodes, the internal quantum efficiency (IQE) of such photodiodes can be predicted and thereby these photodiodes can be used to establish an absolute radiometric scale [1]. The use of biased induced junction photodiodes increases the minority carrier collection efficiency and thereby the IQE as shown by [2] and [3].

A novel type of detector has been developed which is intended to work as a primary standard for radiometry having approximately the same cost, functionality and easy handling as standard transfer detectors. This predictable quantum efficient detector (PQED) presented here is based on custom-made induced junction Si photodiodes. Extensive modelling of the physical effects inside these photodiodes and first experimental characterisations have been carried out [4–8]. The modelling shows that the internal quantum deficiency (IQD[1]) of induced junction photodiodes can be as low as 1 ppm at low temperatures and under reversed bias for the spectral range from 400 nm to 600 nm. For room temperature and reversed bias the IQD is predicted to be in the range of 100 ppm for the whole visible spectral range [5]. Reflection losses are minimised by assembling two photodiodes in a wedge-like trap structure. The beam is reflected seven times before it exits the detector through the entrance aperture (figure 1). Therefore, according to theory and modelling, using this photodiode type in such an assembly enables absolute optical power measurements with an uncertainty of 1 ppm.

The purpose of the measurements presented here was to experimentally validate the modelling of the angular [6] and the polarisation [8] dependence of a room temperature PQED (RT-PQED).

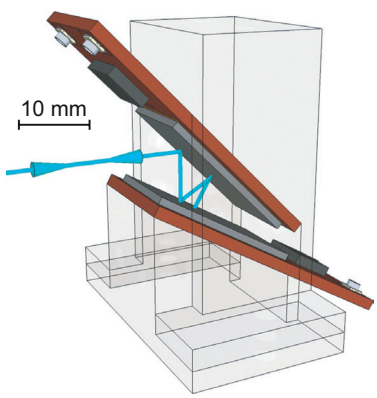

Figure 1: Schematic representation of the PQED's photodiode assembly [6].

[1] IQE = 1 - IQD - *R*, with *R* being reflection losses

2 Angular dependence of the PQED

The purpose of the angular dependence measurements was to validate modelling of the angular response of an RT-PQED published by Sildoja et al. [6]. The measurements were performed at distinct wavelengths and for the *s*- and *p*-polarisation state of the beam. The knowledge of the angular dependent responsivity of an RT-PQED is needed in preparation for measurement applications using non collimated light.

2.1 Measurement setup

The angular dependence measurements were undertaken at the TULIP setup of the PTB [9] using a collimated laser beam. Figure 2 gives a schematic representation of the optical setup.

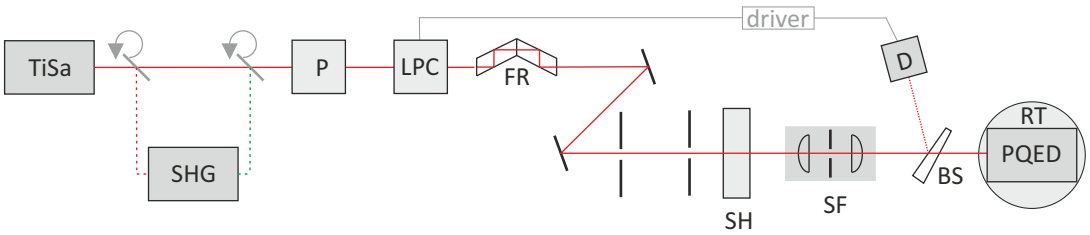

Figure 2: Setup for the angular dependency measurements. TiSa – laser (680 nm, 800 nm), SHG – second harmonic generator (400 nm, 515 nm), P – polariser, LPC – laser power control, FR – Fresnel rhomb ($\lambda/2$ retarder), SH – shutter, SF – spatial filter, BS – beam splitter, D – monitor photodiode, RT – rotation table. The spatial filter was replaced by a lens with $f = 750$ mm for the measurements at 800 nm.

The laser beam was led through a polariser (P) to ensure a highly linear polarisation state. The orientation of the beam polarisation was changed between the *s*- and *p*-state by a Fresnel rhomb (FR). The laser power was stabilised (LPC) using the monitor signal from the photodiode (D). To ensure a collimated and spatially clean beam, the laser beam was led through a spatial filter (SF). The resulting beam radii were in the range from 0.4 mm to 0.6 mm. The PQED was placed onto the rotation table (RT) so that the PQED was rotated around a virtual axis going through the centre of its aperture. Figure 3 gives the allocation of the respective rotational axes. The measurements were undertaken with the angle of incidence spanning a range from -4° to +4° (-3° to +3° in some cases) in steps of 0.5°. Each photodiode was connected to a separate current-to-voltage converter with $U_{\mathrm{BIAS}} = +5$ V. The signals of the two photodiodes were read out simultaneously by two HP 3458 digital voltage meters (DVM).

2.2 Experimental results

2.2.1 Spatial uniformity of the photodiode's responsivity

The spatial uniformity measurements were undertaken with the same setup as used for the angular dependence measurements (figure 2). The RT-PQED was moved along the *x*- and

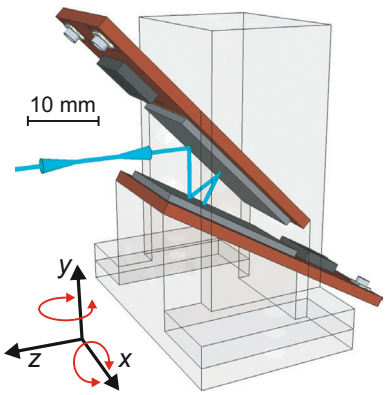

Figure 3: Allocation of the rotation axes with regard to the PQED's photodiode assembly.

y-axes in steps of 1 mm over an area of 10 mm x 10 mm, which approximately equals the aperture of the PQED.
The main purpose of the spatial uniformity measurements was to check for possible contaminations of the photodiode surfaces by dust particles. In the course of the measurements, the spatial uniformity of the PQED turned out to be wavelength dependent. This provided useful information for interpreting also the results from the angular dependence measurements.

According to the measurement results, no contamination of the photodiodes by dust particle occurred during the measurements[2]. Nevertheless, the measurements at the different wavelengths and polarisation states gave significantly different results. For 515 nm and 680 nm the photodiode signals were constant within approximately 100 ppm over a relatively large area. Figure 4 (upper left) gives an example of a scan for 680 nm and a p-polarised beam. The graph gives the sum of the two photodiodes' signals as a function of the x- and y-position. The scans for the s-polarised beam and for 515 nm show comparable behaviour. The scans at 400 nm and at 800 nm, however, delivered rather different results as shown in the other graphs of figure 4. Here, much larger gradients in the spatial responsivity maps were observed. Such behaviour at 400 nm and 800 nm could be caused by inhomogeneities in the oxide layer thickness of the photodiodes.

2.2.2 Measurements of angular dependence

Figures 5 and 6 show the results from the angular dependence measurements. The vertical axis gives the deviation of the summed signals of the two photodiodes from the measurement at 0 °. In some cases shadowing by the RT-PQED housing seemed to appear for the larger displacements, so these data points are masked in the graphs.

[2]The measurements were carried out in a clean room facility and the RT-PQED was constantly flushed with nitrogen during the measurements and sealed when not in use.

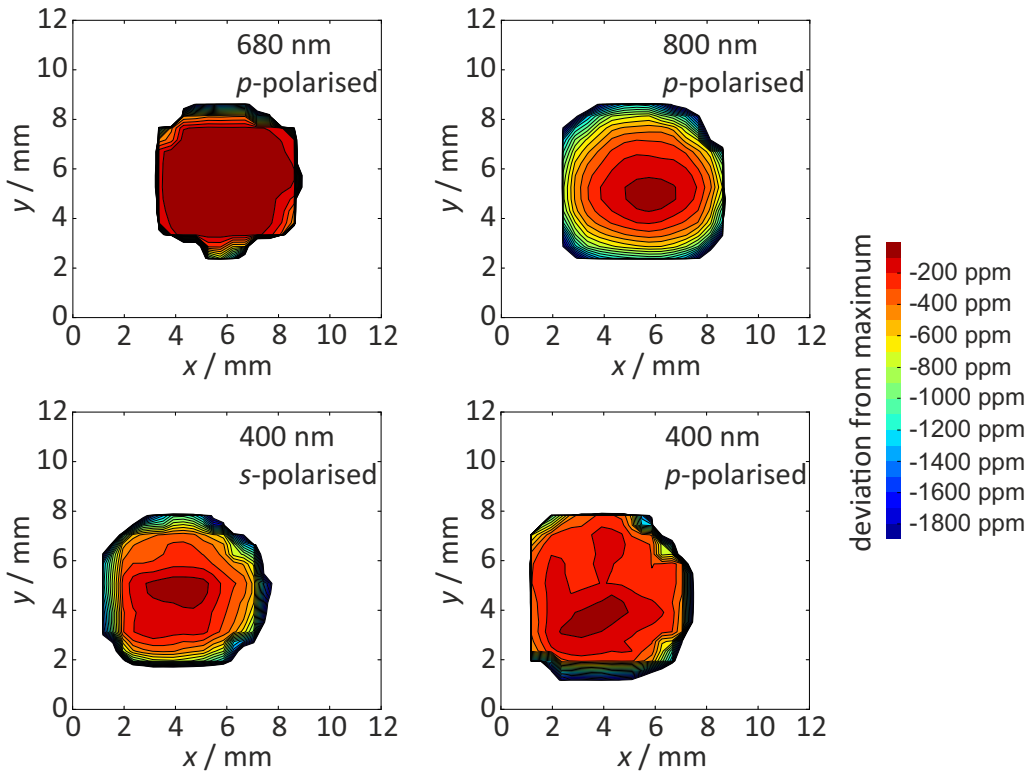

Figure 4: Results from the spatial uniformity scans of the RT-PQED photodiodes.

Measurements at 515 nm and 680 nm: The measurements at 515 nm indicate no angular dependency within the measurement uncertainty. The two outliers at -0.5° and +2° might be caused by inhomogeneities in the oxide layer of the photodiode surface. The measurements at 680 nm also indicate no angular dependency within the measurement uncertainty, except again the outlier at +2°.

Measurements at 400 nm and 800 nm: The results of the measurements at 400 nm and 800 nm wavelength generally showed larger deviations from the 0° measurement as compared to the results at 515 nm and 680 nm wavelengths. The deviations in some cases were slightly larger than 100 ppm and higher than the respective uncertainty values. To interpret these results, the results from the spatial uniformity measurements (figure 4) have to be taken into account. As mentioned in section 2.2.1, the spatial uniformity of the photodiodes' responsivity at 400 nm and 800 nm was worse than the spatial uniformity at 515 nm and 680 nm. When the PQED is rotated, the beam moves on the photodiode surfaces. In the case of measurements at 400 nm and 800 nm the beam would hit areas with different sensitivities. This results in different signals and thereby the larger deviations from the 0° measurements. Therefore the observed angular dependence at 400 nm and 800 nm is probably dominated by variations in the oxide layer thickness rather than by the angular dependence of the reflection as predicted by the modelling [6].

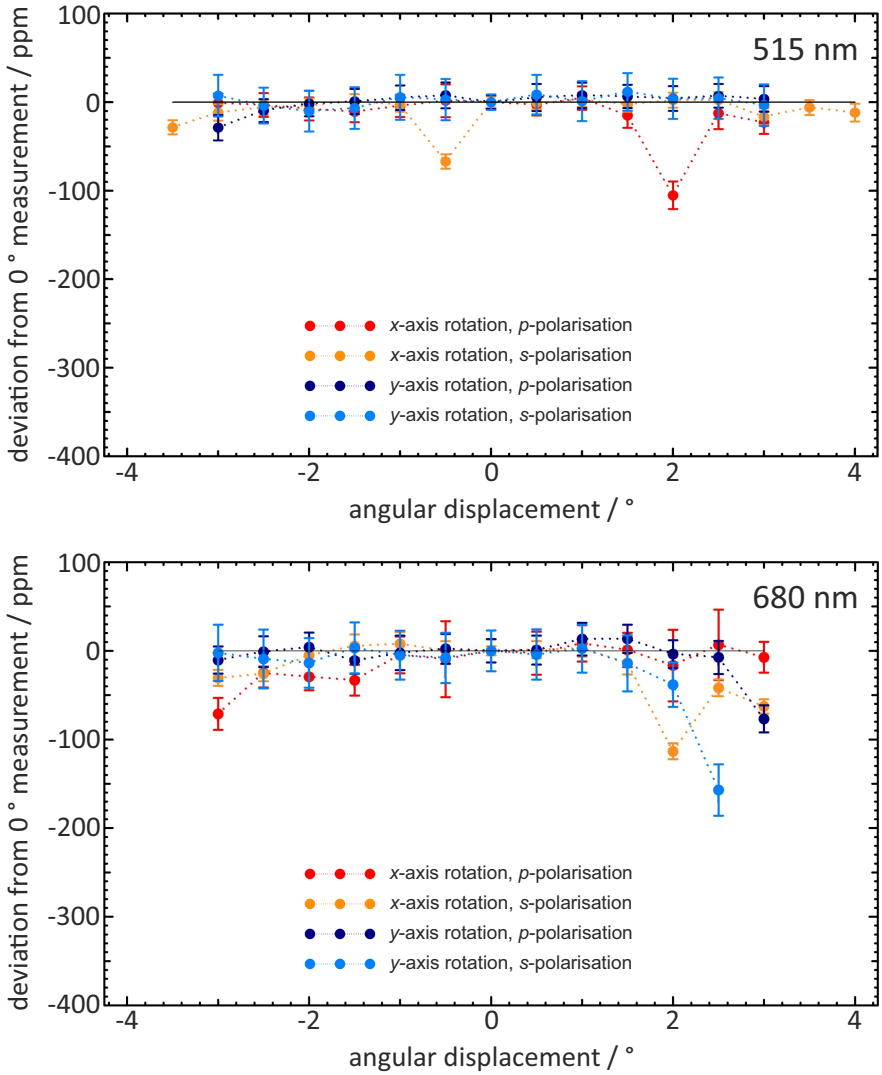

Figure 5: Measurements of angular dependence at $\lambda = 515$ nm and $\lambda = 680$ nm.

2.3 Angular dependence – Overview

The results of the angular dependence measurements of the studied PQED show minor variations that are well within the measurement uncertainties and clearly less than 100 ppm in the mid-visible spectral range (measured at 515 nm and 680 nm). The measurements at 400 nm and 800 nm wavelengths revealed larger variations, though mostly within $\pm$ 100 ppm.

3 Polarisation dependence of the PQED

The purpose of the polarisation dependence measurements was to validate modelling of the RT-PQED behaviour published by Sildoja et al. [8]. The measurements were carried out at distinct wavelengths between 400 nm and 850 nm and for *s*- and *p*-polarisation states of the beam. The knowledge of the polarisation dependent responsivity of an RT-PQED is needed in preparation for measurement applications using non-polarised or partially polarised radiation.

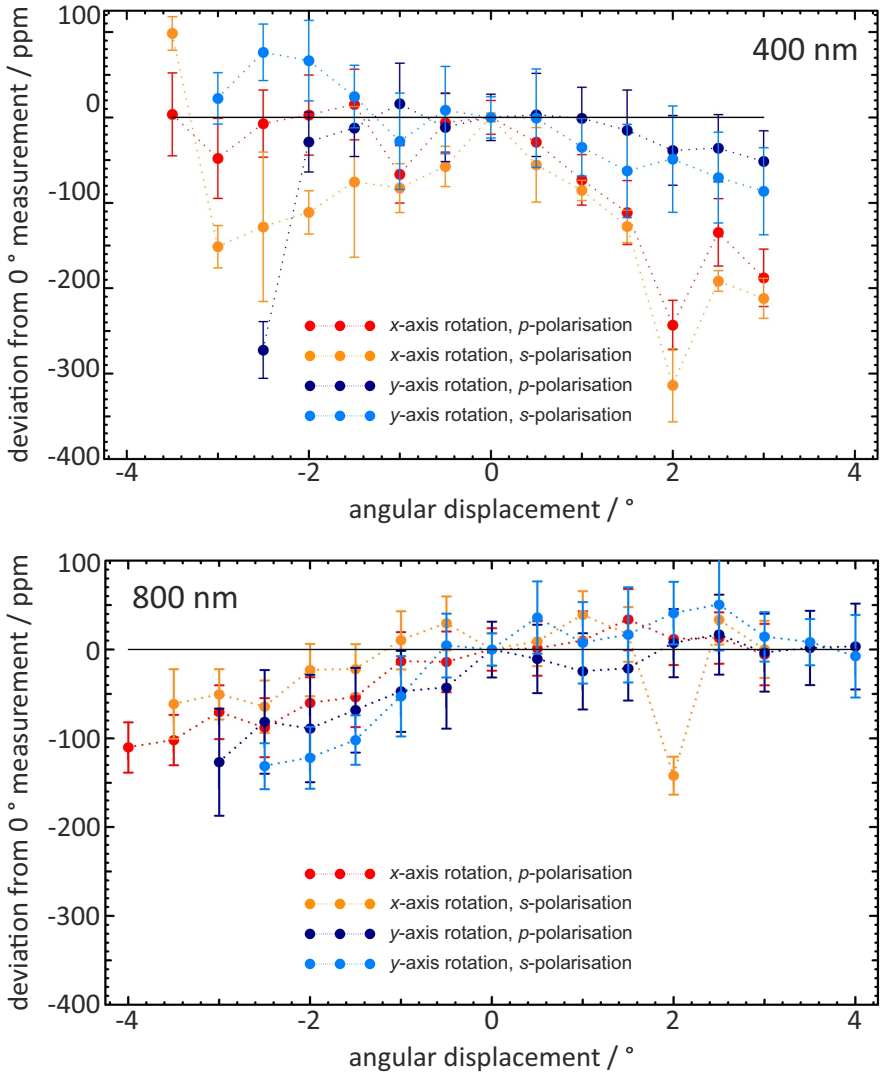

Figure 6: Measurements of angular dependence at $\lambda = 400$ nm and $\lambda = 800$ nm.

3.1 Measurement setup

The polarisation dependence measurements were performed at the TULIP setup of PTB using a slightly focused laser beam. Figure 7 gives a schematic representation of the optical setup. The laser beam was led through a polariser (P) to ensure a highly linear polarisation state. The laser power was stabilised (LPC) using the monitor signal from the photodiode (D). The beam was lead through a lens with $f = 800$ mm to achieve a slight focussing of the beam. The RT-PQED is placed at a certain distance from the focussing lens so the focus of the beam is approximately at the plane of the photodiodes. Each photodiode was connected to a separate current-to-voltage converter with $U_{\mathrm{BIAS}} = +5$ V. The signals of the two photodiodes of the PQED were read out simultaneously by two HP 3458 DVMs.

The RT-PQED was rotated around the z-axis to change its orientation relative to the polarisation of the laser beam from s to p (figure 8, left). To ensure the overlap between the optical axis and the rotation axis, an adjustable rotation unit was designed and built (figure 8,

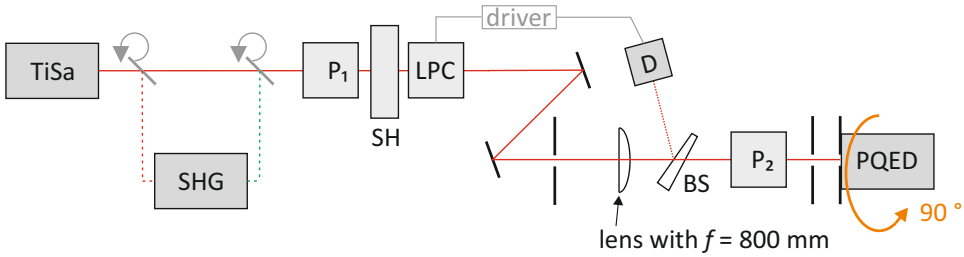

Figure 7: Setup for the polarisation dependence measurements. TiSa – laser (680 nm - 850 nm), SHG – second harmonic generator (400 nm - 500 nm), P – polariser, LPC – laser power control, SH – shutter, BS – beam splitter, D – monitor photodiode. In front of the PQED a precision aperture with a diameter of 5.5 mm was placed.

right). This rather complex setup was necessary because every approach of rotating the polarisation of the beam instead turned out to be inappropriate as the signal intensity reacted very sensitively to even minimal mechanical displacement of the polarisation optic element.

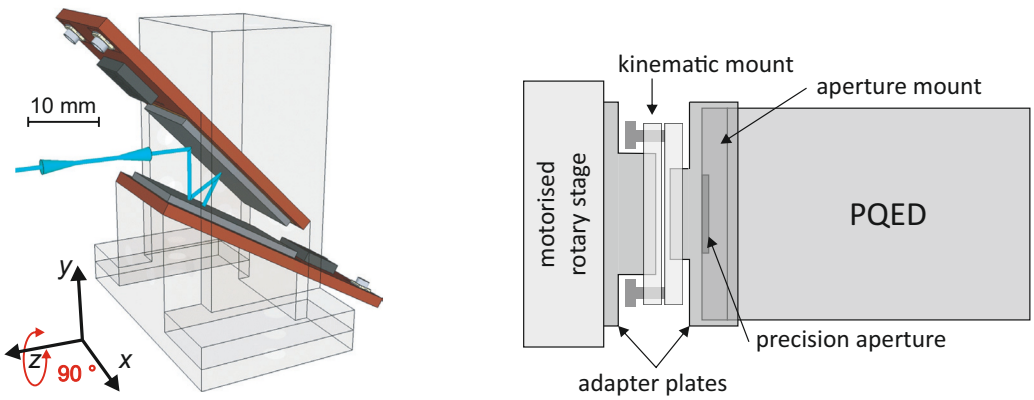

Figure 8: Allocation of the rotation axis for the polarisation dependence measurements (left). Schematic representation of the adjustable rotation unit for automated rotation of the PQED around the optical axis z (right).

3.2 Experimental results

During the measurements the RT-PQED was rotated by at least 90 °, in some cases 110 °. The measurements were carried out at 400 nm, 420 nm, 460 nm, 500 nm, 680 nm, 700 nm, 750 nm, 800 nm and 850 nm.

From the extremes of the course of the single RT-PQED photodiode signals as a function of the PQED rotary position, the polarisation states were assigned. 100 % p-polarisation results in a maximum signal on the photodiode hit first by the beam. The signals from the two photodiodes were summed and the deviation from the measurement with the highest signal ratio between photodiode 1 and 2 was calculated.

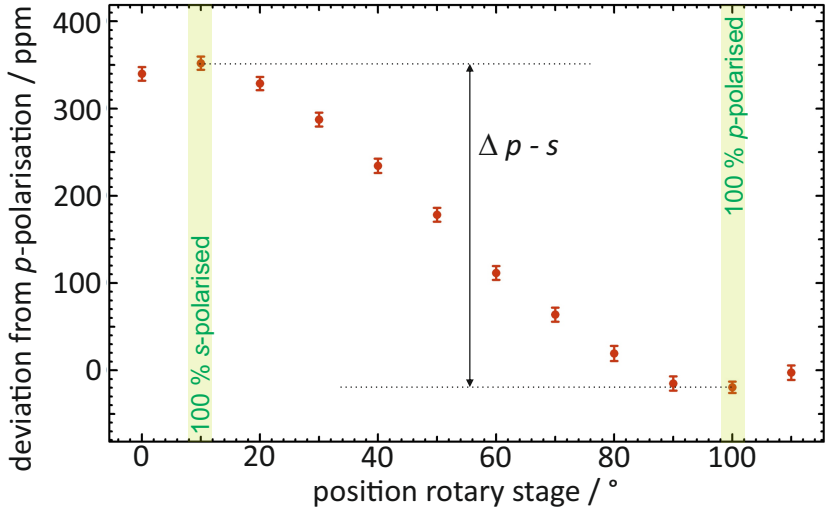

Figure 9: Polarisation dependence measurement at 680 nm.

Figure 9 gives this calculated deviation for the measurement at 680 nm. At the rotary stage position of 10 ° the beam is *s*-polarised, at 100 ° the beam is *p*-polarised. The vertical axis gives the deviation of the signals compared to a measurement with *p*-polarised beam. Δ $p-s$ is the difference between the measurements with the *s*-polarised and the *p*-polarised beam. This value is used for the final analysis shown in figure 10.

The expected values for the difference between the signals for the different polarisation states (figure 10 “model”) are taken from figure 1 in [8] (the underlying numerical data were kindly given to us by the author). As can be seen from figure 10, the experimental results agree well with the modelled values. A possible reason for the higher discrepancy between modelling and experimental data at 400 nm could be the steep increase of the curve which results in higher uncertainty of the overlap between theory and experiment.

3.3 Polarisation dependence - Overview

The experimental results of the polarisation dependence measurements match the expected values based on the modelled reflectance presented in the literature within the 100 ppm uncertainty level aimed at. This experimental validation of the modelled PQED behaviour strongly supports the aim of using the PQED in applications where non-polarised or partially polarised radiation is used.

4 Summary and conclusion

A predicable quantum efficient detector (PQED) for measuring optical power is designed and built and is intended to be used as a primary standard for radiometry. This detector is based on induced junction Si photodiodes with high quantum efficiency. The reflection losses are reduced to a very low level by assembling the photodiodes in a wedge-like trap structure.

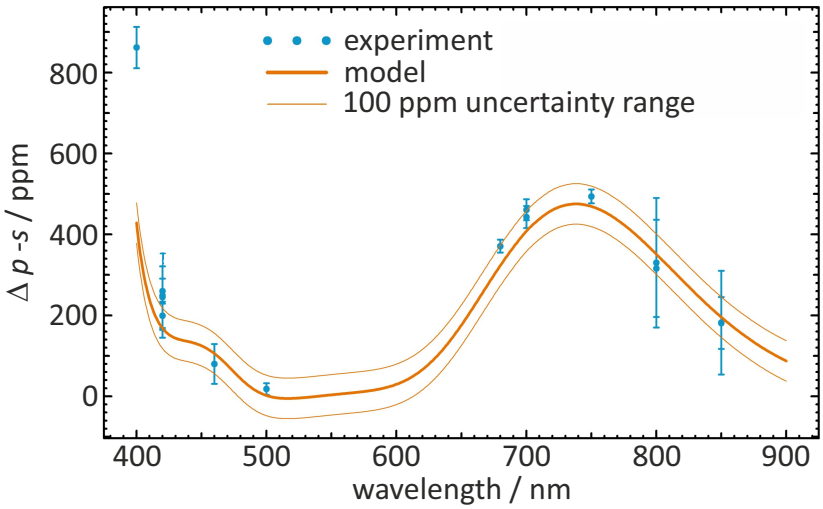

Figure 10: Comparison between experimental values and modelled values for the difference between signals measured with *p*- and *s*-polarised beams.

In this paper results from measurements of the angular and the polarisation dependence of a room-temperature PQED are presented. These results are compared to modelling of the expected PQED behaviour. The measurements of the polarisation dependence correspond to the modelled behaviour within 100 ppm uncertainty. The angular dependence is negligibly low in the medium range of the visible spectrum. Measurements at 400 nm and 800 nm showed angular dependencies slightly exceeding the 100 ppm level. Nevertheless, the results presented here and their comparison to modelled values are promising regarding the aim of developing a new primary standard for radiometry.

Acknowledgements
Part of this work has been supported by the European Metrology Research Programme (EMRP) within the joint research project “New primary standards and traceability for radiometry (NEWSTAR)”. The EMRP is jointly funded by the EMRP participating countries within EURAMET and the European Union.

References

[1] Jon Geist. Quantum efficiency of the p-n junction in silicon as an absolute radiometric standard. *Applied Optics*, 18:760 – 762, 1979.

[2] T. E. Hansen. Silicon UV-photodiodes using natural inversion layers. *Physica Scripta*, 18:471 – 475, 1978.

[3] Jon Geist, Eli Liang, and A. Russel Schaefer. Complete collection of minority carriers from the inversion layer in induced junction diodes. *Journal of Applied Physics*, 52:4879 – 4881, 1981.

[4] Meelis Sildoja, Farshid Manoocheri, and Erkki Ikonen. Reflectance calculations for a predictable quantum efficient detector. *Metrologia*, 46:151 – 154, 2009.

[5] Jarle Gran, Toomas Kübarsepp, Meelis Sildoja, Farshid Manoocheri, Erkki Ikonen, and Ingmar Müller. Simulations of a predictable quantum efficient detector with PC1D. *Metrologia*, 49:130 – 134, 2012.

[6] Meelis Sildoja, Farshid Manoocheri, Mikko Merimaa, Erkki Ikonen, Ingmar Müller, Lutz Werner, Jarle Gran, Toomas Kübarsepp, Marek Smîd, and Maria Luisa Rastello. Predictable quantum efficient detector: I. Photodiodes and predicted responsivity. *Metrologia*, 50:385 – 394, 2013.

[7] Ingmar Müller, Uwe Johannsen, Ulrike Linke, Liana Socaciu-Siebert, Marek Smîd, Geiland Porrovecchio, Meelis Sildoja, Farshid Manoocheri, Erkki Ikonen, Jarle Gran, Toomas Kübarsepp, Giorgio Brida, and Lutz Werner. Predictable quantum efficient detector: II Characterization and confirmed responsivity. *Metrologia*, 50:395 – 401, 2013.

[8] Meelis Sildoja, Timo Dönsberg, Henrik Mäntynen, Mikko Merimaa, Farshid Manoocheri, and Erkki Ikonen. Use of the predictable quantum efficient detector with light sources of uncontrolled state of polarization. *Measurement Science and Technology*, 25, 2014.

[9] Michaela Schuster, Saulius Nevas, Armin Sperling, and Stephan Völker. Spectral calibration of radiometric sources using tunable laser sources. *Applied Optics*, 51:1950 – 1961, 2012.